Finite-temperature strong-coupling expansions for the Kondo lattice model

J. Oitmaa* and Weihong Zheng[†]

School of Physics, The University of New South Wales, Sydney, NSW 2052, Australia
(Received 11 September 2002; published 6 June 2003)

Strong-coupling expansions, to order $(t/J)^8$, are derived for the Kondo lattice model of strongly correlated electrons, in one, two, and three dimensions at an arbitrary temperature. Results are presented for the specific heat, and spin and charge susceptibilities.

I. INTRODUCTION

This paper, the second of a sequence, studies the thermodynamic properties of the Kondo lattice model, described by the Hamiltonian

$$H = -t \sum_{\langle ij \rangle \sigma} (c_{i\sigma}^{\dagger} c_{j\sigma} + \text{H.c.}) + J \sum_i \mathbf{S}_i \cdot \mathbf{s}_i - \mu \sum_{i\sigma} n_{i\sigma}. \quad (1)$$

The first term describes a single band of conduction electrons, the "Kondo coupling" term represents an exchange interaction between conduction electrons and a set of localized $S = \frac{1}{2}$ spins, and the final term allows for variable conduction electron density via a chemical potential.

The Kondo lattice model combines two competing physical effects. In the strong coupling (large $|J|$) limit, the conduction electrons will form local singlets ($J > 0$) or triplets ($J < 0$) with the localized spin at each site. In either case there will be a gap to spin excitations and spin correlations will be short ranged. On the other hand, at weak coupling, the conduction electrons can induce the usual RKKY interaction between localized spins, leading to magnetic order.

The antiferromagnetic model is believed to be relevant to heavy-electron systems such as $CeCu_{6-x}Au_x$,[1] where non-Fermi liquid behavior is observed near a quantum critical point. A popular scenario[2] is that low-energy spin fluctuations, as represented by the Kondo lattice model, are an essential part of the physics of these systems. While we do not address this connection here, it is hoped that our results will be of interest in this context.

Despite the apparent simplicity of the model, no exact results are known, either at $T = 0$ or at finite temperatures, in any spatial dimension. In the preceding paper,[3] we studied the ground-state properties of the model at $T = 0$, using linked-cluster series expansions. We refer to that paper for a discussion on other work, which has been, almost exclusively, restricted also to $T = 0$. In the present paper, we focus on finite-temperature thermodynamic properties. We know of only a few previous studies of this kind. Röder *et al.*[4] considered the ferromagnetic model in the limit $J \to -\infty$, on the simple cubic lattice, via a high-temperature expansion. Here, we treat the general J case and focus on the antiferromagnetic model. Shibata *et al.*[5] have studied the one-dimensional (1D) antiferromagnetic model via a finite-temperature density matrix renormalization group (DMRG) approach. Haule *et al.*[6] have treated the 2D case, primarily via a numerical finite-temperature Lanczos method. We compare our results

with this work wherever possible. Haule *et al.* have also considered the atomic limit ($t = 0$), and the order t^2 correction terms. Our work was largely motivated by this paper.

Our approach, which will be described in the following section, treats the single-site terms exactly and treats the hopping term perturbatively. It is, thus, an expansion about the "atomic limit." We summarize here, for completeness and for later reference, the exact results in this limit.

For variable conduction electron density, there are eight states per site: two states with no conduction electrons and localized spin up or down, two states with two conduction electrons of opposite spins, and two states (one singlet and three triplets) with one conduction electron coupled to the localized spin. For a lattice of N sites, the grand partition function is

$$\mathcal{Z}_0 \equiv \text{Tr}\{e^{-\beta H}\} = z_0^N \quad (2)$$

with

$$z_0 = 2 + (e^{3K} + 3e^{-K})\zeta + 2\zeta^2 \quad (3)$$

and $K \equiv \beta J/4$, $\zeta = e^{\beta\mu}$, $\beta = 1/k_B T$.

The internal energy per site is given by

$$u(\zeta, T) = -\left. \frac{\partial}{\partial \beta} \right|_{\zeta} \ln z_0 = \frac{-\frac{3}{4}J(e^{3K} - e^{-K})\zeta}{2 + (e^{3K} + 3e^{-K})\zeta + 2\zeta^2}. \quad (4)$$

The fugacity can, as usual, be eliminated in favor of the electron density n by using the relation

$$n(\zeta, T) = \zeta \left. \frac{\partial}{\partial \zeta} \right|_T \ln z_0 = \frac{q\zeta + 2\zeta^2}{1 + q\zeta + \zeta^2}, \quad (5)$$

where we have introduced $q \equiv \frac{1}{2}(e^{3K} + 3e^{-K})$. Solving this gives

$$\zeta = \frac{-q(1-n) + \sqrt{q^2(1-n)^2 + 4n(2-n)}}{2(2-n)}. \quad (6)$$

The specific heat is then obtained from Eqs. (4) and (6) via the usual relation $C_v = du/dT$.

Also of interest are the compressibility or "charge susceptibility"

$$\chi_c = \frac{\partial n}{\partial \mu}, \quad (7)$$

which can be expressed as

$$\beta^{-1}\chi_c = \frac{q(1-n)\zeta + 2(2-n)\zeta^2}{1+q\zeta+\zeta^2} \quad (8)$$

and the magnetic susceptibility, which is given by

$$4\beta^{-1}\chi_s = \frac{1+4e^{-K}\zeta+\zeta^2}{1+q\zeta+\zeta^2}. \quad (9)$$

Simpler analytic results can be obtained in various limits: at high or low temperature, and at or near half filling. Some of these are given in Ref. 6, although these contain minor errors in a few cases.

Of course, in the atomic limit, all of these quantities are smooth functions of temperature and electron density.

II. THERMODYNAMIC PERTURBATION THEORY

Our goal is to obtain an expression for the thermodynamic potential, and hence other quantities, in powers of t/J. We work in the grand canonical ensemble and write the Hamiltonian as

$$H = H_0 + V \quad (10)$$

with

$$H_0 = J\sum_i \mathbf{S}_i \cdot \mathbf{s}_i - \mu \sum_{i\sigma} n_{i\sigma}, \quad (11)$$

$$V = -t\sum_{\langle ij\rangle\sigma} (c_{i\sigma}^\dagger c_{j\sigma} + \text{H.c.}). \quad (12)$$

The grand partition function can then be expanded in the usual way as

$$\mathcal{Z}_g = \text{Tr}\{e^{-\beta(H_0+V)}\}$$

$$= \mathcal{Z}_0 \left\{ 1 + \sum_{r=1}^\infty (-1)^r \right.$$

$$\left. \times \int_0^\beta d\tau_1 \cdots \int_0^{\tau_{r-1}} d\tau_r \langle \tilde{V}(\tau_1)\cdots\tilde{V}(\tau_r)\rangle \right\} \quad (13)$$

with

$$\tilde{V}(\tau) = e^{\tau H_0}Ve^{-\tau H_0} \quad (14)$$

and

$$\langle A\rangle = \frac{1}{\mathcal{Z}_0}\text{Tr}\{e^{-\beta H_0}A\}, \quad (15)$$

where $\mathcal{Z}_0$ is the atomic limit partition function (2). The free energy (grand potential) is then given by

$$-\beta F = N\ln z_0 + \sum_{r=1}^\infty (-1)^r T_r, \quad (16)$$

where

$$T_r = \int_0^\beta d\tau_1 \cdots \int_0^{\tau_{r-1}} d\tau_r \langle \tilde{V}(\tau_1)\cdots\tilde{V}(\tau_r)\rangle_N \quad (17)$$

and the subscript N signifies that only the part proportional to N is to be included.

This approach is, of course, well known and has been used in the past for both pure spin models[7] and for the Hubbard model.[8] Any contribution to T_r in Eq. (17) comes from a particular cluster of sites and bonds, a "graph." It is possible to restrict the class of graphs to connected ones only, as done in Ref. 7. In our work we also included disconnected graphs, of more than one component, as these are rather easy to deal with directly. Since each bond contributes a $\tilde{V}$ operator and hence a factor t, it is obvious that to carry the expansion to order t^r, all topologically distinct graphs with up to r bonds need to be considered. There are a total of 115 graphs through eighth order, which is as far as we have been able to compute. Technically, these are multigraphs with all vertices of even degrees. Many bare graphs with eight edges do not contribute at this order.

The contribution of a particular graph G to the free energy can be expressed in the form

$$T_r(G) = C_G(t/J)^r z_0^{-p} \sum_{s,l,m} a_{s,l,m}K^l e^{mK}\zeta^s, \quad (18)$$

where C_G is the embedding factor, or "weak lattice constant" of graph G in the particular lattice considered, p is the number of points or vertices in the graph, the $a_{s,l,m}$ are numerical constants, and the sum contains, for each graph, a finite set of terms labeled by integers s,l,m. Evaluation of these expressions is a lengthy procedure, involving a trace over a space of 8^p states and evaluation, for each term in the trace, of an r-fold multiple integral. It is possible to find many time saving refinements, but, even so, the evaluation of the worst case, the octagon, took about 260 h of CPU time on a 1 GHz Compaq alpha processor.

Having computed the $T(G)$ factors for all graphs, it is then a simple matter to combine these and to obtain, for any lattice, the free energy per site in the form

$$-\beta f = \ln z_0 + \sum_{r=2}^\infty z_0^{-r}F_r(K,\zeta)(t/J)^r, \quad (19)$$

where the F_r are complete expressions in K and ζ of the form

$$F_r(K,\zeta) = \sum_{s,l,m} a_{s,l,m}K^l e^{mK}\zeta^s. \quad (20)$$

These expressions are too lengthy to display here, but can be supplied on request. To give some idea of the size, the eighth order factor F_8 contains 1042 separate terms.

From Eqs. (19) and (20), one can compute expressions for the internal energy and specific heat. The internal energy can be expressed in the form

$$u = -\frac{\partial}{\partial \beta}\big|_\zeta(-\beta f) = u_0 + \sum_{r=2}^{\infty} z_0^{-(r+1)} E_r(K, \zeta)(t/J)^r,$$
(21)

where u_0 is the atomic limit result (4) and the $E_r(K, \zeta)$ are complete expressions. The specific heat is $C_v = du/dT$. For most purposes, it is more useful to express the series in terms of electron density n, which can be obtained from Eq. (19) via

$$n = \zeta \frac{\partial}{\partial \zeta}(-\beta f) = n_0 + \sum_{r=2}^{\infty} z_0^{-(r+1)} Y_r(K, \zeta)(t/J)^r,$$
(22)

where n_0 is the atomic limit result (5) and the $Y_r(K, \zeta)$ are, again, complete expressions in K, ζ. For fixed n and K we then use a numerical reversion procedure to obtain expansions for the fugacity, in power of t/J, which can then be eliminated from the thermodynamic functions. For half filling ($n=1$), this reversion can be carried out analytically.

In addition, we have included a magnetic-field term

$$H' = H - h\sum (n_{i,\uparrow} - n_{i,\downarrow} + 2S_i^z)$$
(23)

to allow calculation of the zero-field magnetic susceptibility χ_s, which is expressed in the form

$$\beta^{-1}\chi_s = \beta^{-1}\chi_0 + \sum_{r=2}^{\infty} z_0^{-(r+1)} X_r(K, \zeta)(t/J)^r,$$
(24)

where, again, the first term is the atomic limit result (9) and the X_r are complete expressions. The fugacity can again be eliminated in favor of the electron density, as described above.

Several checks on the correctness of our results have been made. Since temperature enters explicitly, we can take the zero-temperature ($K \to \infty$) limit analytically, to recover the ground-state energy series.[3,9] Another test is the $J \to 0$ limit, in which $F_r(K, \zeta)$ in Eq. (19) has a leading term of order K^r, giving an expression in powers of βt. This can be compared with the results for free electrons. A complete agreement is obtained. We are confident that our results are correct, but cannot exclude the possibility of errors not picked up by these checks.

The analysis of the results follows standard lines. For any fixed K, ζ, we obtain expressions for thermodynamic quantities as a series in the single variable t/J. For small t/J, the series converges rapidly and even a naive sum gives a good accuracy. Padé approximants and integrated differential approximants[11] allow extrapolation to larger t/J. For fixed n we obtain series for ζ in terms of t/J, which are then substituted into corresponding expressions (20) and (24) to obtain a single-variable series in t/J, which is then evaluated as before. To calculate the specific heat, it is necessary to include derivatives of ζ with respect to temperature. For the

benefit of the reader, we give in Table I coefficients for some representative cases. Other series can be supplied on request.

While the general expressions are too lengthy to write down, at high temperatures, one can expand the various quantities in powers of β or K. The expressions up to order K^4 are provided in the Appendix. These are valid for all loose-packed/bipartite lattices.

In the following sections, we present results for the linear chain, the square lattice, and the simple cubic lattice. A discussion of other lattices will be presented elsewhere.

III. THE 1D KONDO LATTICE MODEL

We consider the antiferromagnetic model on a linear chain, with an arbitrary electron concentration n. Using the procedure described above, we have computed the specific heat and spin and charge susceptibilities. Figures 1(a)-1(c) show these quantities, as functions of temperature, at $n=1$ (half filling) for $t/J = 0, 0.2, 0.4, 0.5, 0.6$. For $t/J \lesssim 0.4$, the series are well converged and the curves are obtained simply from the partial sums. For the larger values integrated differential approximants have been used, with the error bars indicating the variation between different approximants. A good agreement is obtained with the DMRG results for all three quantities. However, our (relatively short) series are unable to probe the larger t/J region as well as DMRG can.

Some comments on Fig. 1 are in order. Figure 1(a) shows the specific heat, which shows an interesting crossover from a single peak for small t to a two-peak structure at larger t. In the larger t region, the high-temperature peak becomes broadened and less prominent and is, presumably, due to conduction electrons, whereas the low-temperature peak arises from the fluctuating local spins. The spin susceptibility [Fig. 1(b)] also has a peak at a characteristic temperature. The peak is enhanced and moves to lower T on increasing the hopping parameter t. Increasing t/J will weaken the singlet correlations, and a lower characteristic temperature is sufficient for thermal fluctuations to become dominant. There is some indication of a double peak for $t/J = 0.6$, but this may be an artifact of the numerical analysis. The charge susceptibility also has a peak at the characteristic temperature, and a rapid drop to zero at low temperatures. The peak is depressed with increasing t, but the position stays relatively constant.

To display the effect of varying conduction electron density we have chosen an intermediate value $t/J = 0.4$ and show, in Figs. 2(a)–2(c), curves of C_v, χ_s, and χ_c versus temperature for $n=1$, 0.75, 0.5, and 0.25. The high-temperature peak in C_v [Fig. 2(a)] drops roughly proportionally to n, in agreement with the assignment of this peak to conduction electrons. The series do not allow the low-T specific heat to be determined with sufficient precision to see the effects of doping. Tsunetsugu et al.[10] present a ground-state phase diagram of the 1D Kondo lattice (Fig. 6 of Ref. 10), where a transition line separates a small n ferromagnetic phase from a large n paramagnetic phase. For the parameter ratio $t/J = 0.4$, the critical doping is $n_c \simeq 0.65$. While there

TABLE I. Series coefficients for the internal energy u, specific heat C_v, magnetic susceptibility χ_s, and charge magnetic susceptibility χ_c at $\beta J = 1$ and electron densities $n = 1, 0.5$ for the linear chain, the square lattice, and the simple cubic lattice. Nonzero coefficients $(t/J)^r$ up to order $r = 8$ are listed.

	Linear chain		Square lattice		Simple cubic lattice	
r	$n=1$	$n=0.5$	$n=1$	$n=0.5$	$n=1$	$n=0.5$
			u/J			
0	$-1.187\,272\,75\times10^{-1}$	$-8.781\,925\,21\times10^{-2}$	$-1.187\,272\,75\times10^{-1}$	$-8.781\,925\,21\times10^{-2}$	$-1.187\,272\,75\times10^{-1}$	$-8.781\,925\,21\times10^{-2}$
2	$-9.190\,836\,67\times10^{-1}$	$-6.904\,883\,88\times10^{-1}$	$-1.838\,167\,33$	$-1.380\,976\,78$	$-2.757\,251\,00$	$-2.071\,465\,16$
4	$2.021\,668\,68\times10^{-1}$	$1.941\,565\,99\times10^{-1}$	$1.239\,454\,60$	$8.511\,333\,43\times10^{-1}$	$3.111\,863\,19$	$1.970\,930\,23$
6	$-5.813\,168\,38\times10^{-2}$	$-6.823\,522\,22\times10^{-2}$	$-1.245\,407\,59$	$-8.520\,578\,57\times10^{-1}$	$-5.900\,667\,30$	$-2.950\,786\,62$
8	$1.714\,264\,15\times10^{-2}$	$2.256\,626\,66\times10^{-2}$	$1.388\,764\,32$	$9.812\,273\,89\times10^{-1}$	$1.321\,490\,47\times10^{1}$	$5.069\,622\,22$
			C_v/k_B			
0	$1.440\,457\,99\times10^{-1}$	$1.039\,101\,38\times10^{-1}$	$1.440\,457\,99\times10^{-1}$	$1.039\,101\,38\times10^{-1}$	$1.440\,457\,99\times10^{-1}$	$1.039\,101\,38\times10^{-1}$
2	$7.423\,550\,42\times10^{-1}$	$5.629\,691\,88\times10^{-1}$	$1.484\,710\,08$	$1.125\,938\,38$	$2.227\,065\,13$	$1.688\,907\,57$
4	$-5.053\,804\,30\times10^{-1}$	$-4.993\,487\,45\times10^{-1}$	$-3.168\,639\,38$	$-2.181\,705\,64$	$-7.989\,776\,84$	$-5.047\,070\,69$
6	$2.395\,753\,11\times10^{-1}$	$2.944\,841\,97\times10^{-1}$	$5.372\,973\,55$	$3.704\,600\,27$	$2.575\,217\,20\times10^{1}$	$1.274\,791\,26\times10^{1}$
8	$-9.618\,394\,14\times10^{-2}$	$-1.348\,122\,80\times10^{-1}$	$-8.407\,262\,63$	$-6.027\,876\,17$	$-8.150\,893\,18\times10^{1}$	$-3.077\,847\,24\times10^{1}$
			$\beta^{-1}\chi_s$			
0	$3.025\,529\,20\times10^{-1}$	$2.888\,719\,28\times10^{-1}$	$3.025\,529\,20\times10^{-1}$	$2.888\,719\,28\times10^{-1}$	$3.025\,529\,20\times10^{-1}$	$2.888\,719\,28\times10^{-1}$
2	$-2.693\,465\,03\times10^{-2}$	$-1.341\,190\,52\times10^{-2}$	$-5.386\,930\,06\times10^{-2}$	$-2.682\,381\,04\times10^{-2}$	$-8.080\,395\,10\times10^{-2}$	$-4.023\,571\,57\times10^{-2}$
4	$1.338\,589\,87\times10^{-2}$	$7.419\,337\,27\times10^{-3}$	$8.146\,932\,83\times10^{-2}$	$2.593\,216\,63\times10^{-2}$	$2.042\,502\,89\times10^{-1}$	$5.553\,848\,70\times10^{-2}$
6	$-6.152\,303\,77\times10^{-3}$	$-3.941\,947\,96\times10^{-3}$	$-1.258\,468\,11\times10^{-1}$	$-2.899\,789\,05\times10^{-2}$	$-5.889\,728\,72\times10^{-1}$	$-5.653\,491\,37\times10^{-2}$
8	$2.690\,699\,27\times10^{-3}$	$1.925\,502\,52\times10^{-3}$	$1.940\,268\,24\times10^{-1}$	$3.560\,788\,18\times10^{-2}$	$1.787\,799\,22\times10^{0}$	$-3.464\,099\,64\times10^{-2}$
			$\beta^{-1}\chi_c$			
0	$4.731\,822\,56\times10^{-1}$	$3.603\,276\,15\times10^{-1}$	$4.731\,822\,56\times10^{-1}$	$3.603\,276\,15\times10^{-1}$	$4.731\,822\,56\times10^{-1}$	$3.603\,276\,15\times10^{-1}$
2	$-2.147\,521\,62\times10^{-1}$	$-1.249\,474\,46\times10^{-1}$	$-4.295\,043\,23\times10^{-1}$	$-2.498\,948\,93\times10^{-1}$	$-6.442\,564\,85\times10^{-1}$	$-3.748\,423\,39\times10^{-1}$
4	$9.574\,364\,01\times10^{-2}$	$6.512\,836\,84\times10^{-2}$	$5.889\,841\,98\times10^{-1}$	$2.452\,254\,49\times10^{-1}$	$1.479\,721\,67$	$5.402\,912\,43\times10^{-1}$
6	$-3.932\,490\,95\times10^{-2}$	$-3.258\,454\,79\times10^{-2}$	$-8.442\,345\,59\times10^{-1}$	$-2.816\,505\,91\times10^{-1}$	$-4.003\,014\,87$	$-7.064\,398\,79\times10^{-1}$
8	$1.515\,545\,30\times10^{-2}$	$1.499\,960\,60\times10^{-2}$	$1.220\,353\,14$	$3.566\,654\,68\times10^{-1}$	$1.160\,336\,53\times10^{1}$	$5.017\,503\,66\times10^{-1}$

cannot be true order at a finite temperature, the marked change in the low-T specific heat between the two curves with $n = 0.75$ and 0.5 may will be a reflection of this effect. The effect of doping on χ_s is dramatic. For $n = 1$, at low temperatures, the system is in a gapped singlet phase and χ_s goes to zero exponentially. Away from half-filling, there will be free spins and χ_s diverges according to the usual Curie law. The charge susceptibility χ_c also shows a sharp cross-over between the undoped and the doped cases. The 1D results are consistent with the, presumably, more accurate DMRG calculations. We are not aware of any published DMRG results for specific heat at finite doping, or for the susceptibility for $n < 0.8$. Our results confirm that the series approach can be successfully applied to this model. We now
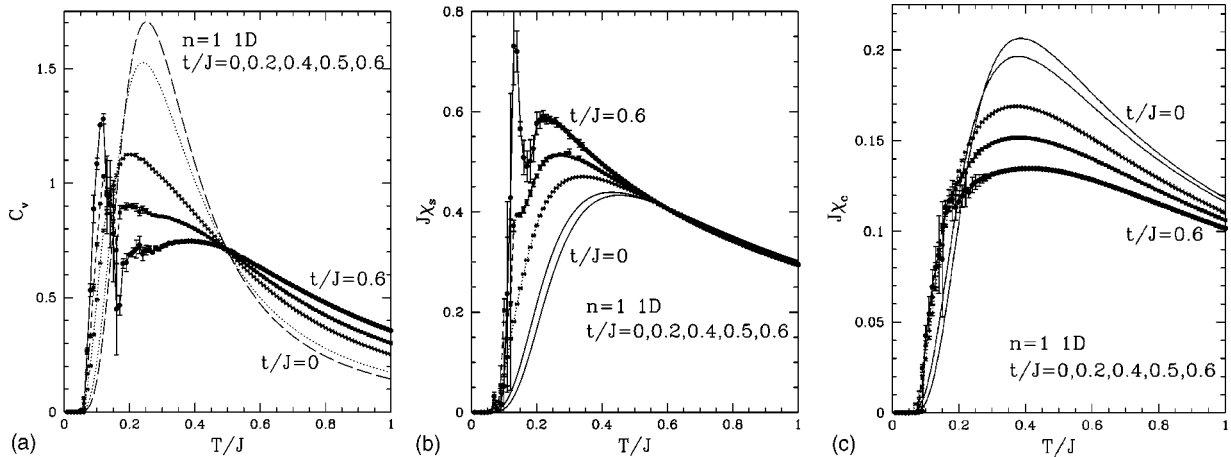
FIG. 1. The specific heat C_v (a), magnetic susceptibility χ_s (b), and charge susceptibility χ_c (c) vs T/J for the linear chain at $n = 1$ for $t/J = 0, 0.2, 0.4, 0.5$, and 0.6.
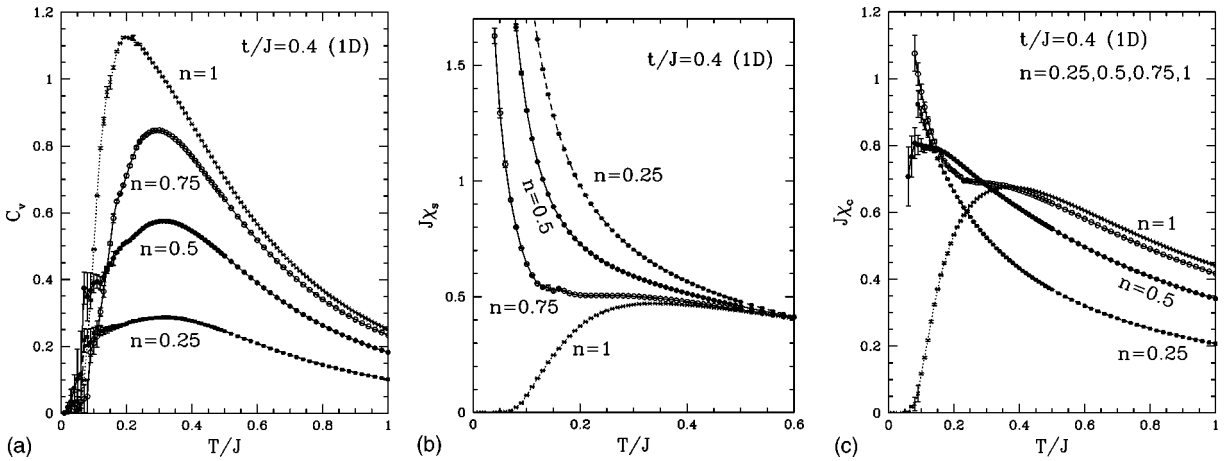
FIG. 2. The same as Fig.1, but for $t/J=0.4$ and $n=1,0.75,0.5,0.25$.

turn to the 2D and 3D cases, where far less is known and where other methods have particular difficulties.

IV. THE 2D AND 3D SYSTEMS

We have computed and analyzed series for the specific heat, spin susceptibility, and charge susceptibility for both the square and simple cubic lattices. Some representative series are given in Table I. We choose to present results for the two lattices together so as to highlight similarities and differences between them.

Figure 3 shows the specific heat at half filling for various t/J ratios. The qualitative behavior is similar to the 1D case, although smaller values of t/J suffice to produce comparable deviations from the atomic limit. A two-peak structure is manifest at $t/J=0.4$. Figure 4 shows the dependence of the specific heat on doping (for fixed $t/J=0.3$). The decrease with decreasing n again confirms that the high-T specific heat is due to conduction electrons. Figures 5 and 6 show the magnetic susceptibility, at half filling for various t/J ratios and at $t/J=0.3$ for various electron densities. Figure 6 shows a stricking crossover from $n=1$, where χ_s is structureless and vanishes as $T\rightarrow 0$, to lower densities $n=0.5$ and 0.25, where χ_s appears to diverge. Evidently, $n=0.75$ is near the critical concentration, as χ_s appears to start to diverge but then drops to zero. There is also some apparent structure for the 3D case at $T/J\simeq 0.15$, which may be an artifact of the analysis.

A mean-field treatment[10] suggests the existence of a finite-temperature phase transition to a ferromagnetic phase for small n, at least for the 3D case. To explore this, we plot the inverse susceptibility versus T in Figure 7. For both lat-
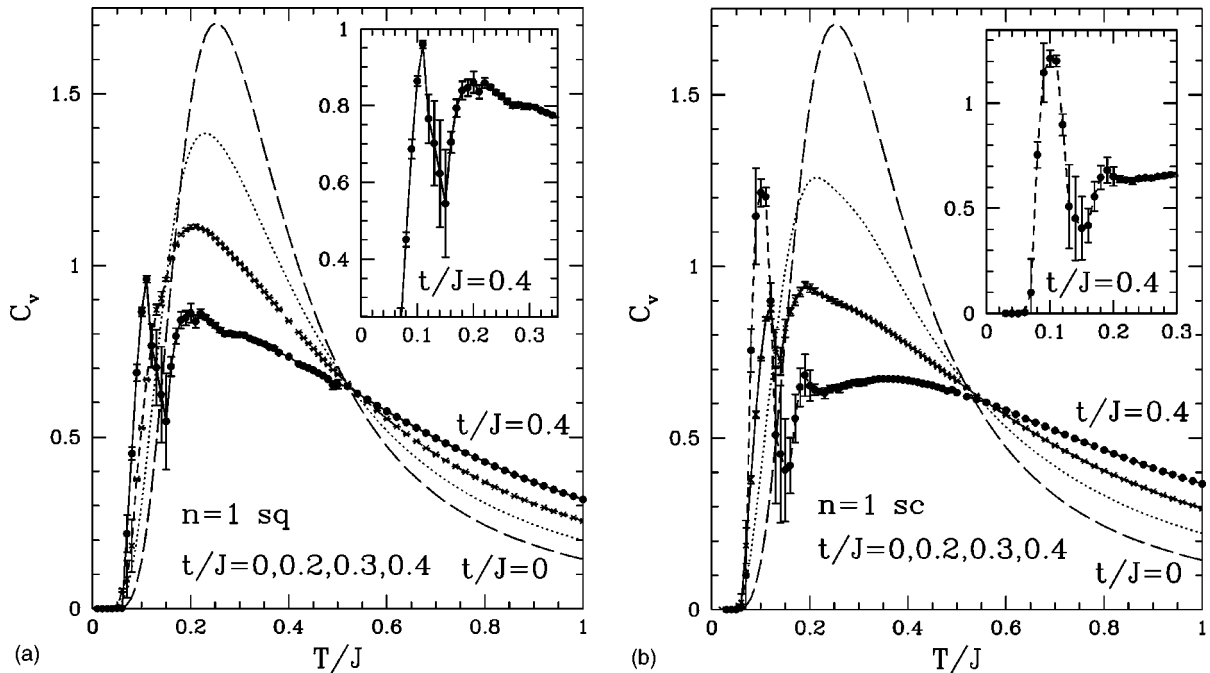
FIG. 3. The specific heat C_v vs T/J for square lattice (sq) (a) and simple cubic lattice (sc) (b) at $n=1$ for $t/J=0$, 0.2, 0.3, and 0.4. The insets enlarge the small T/J region for $t/J=0.4$
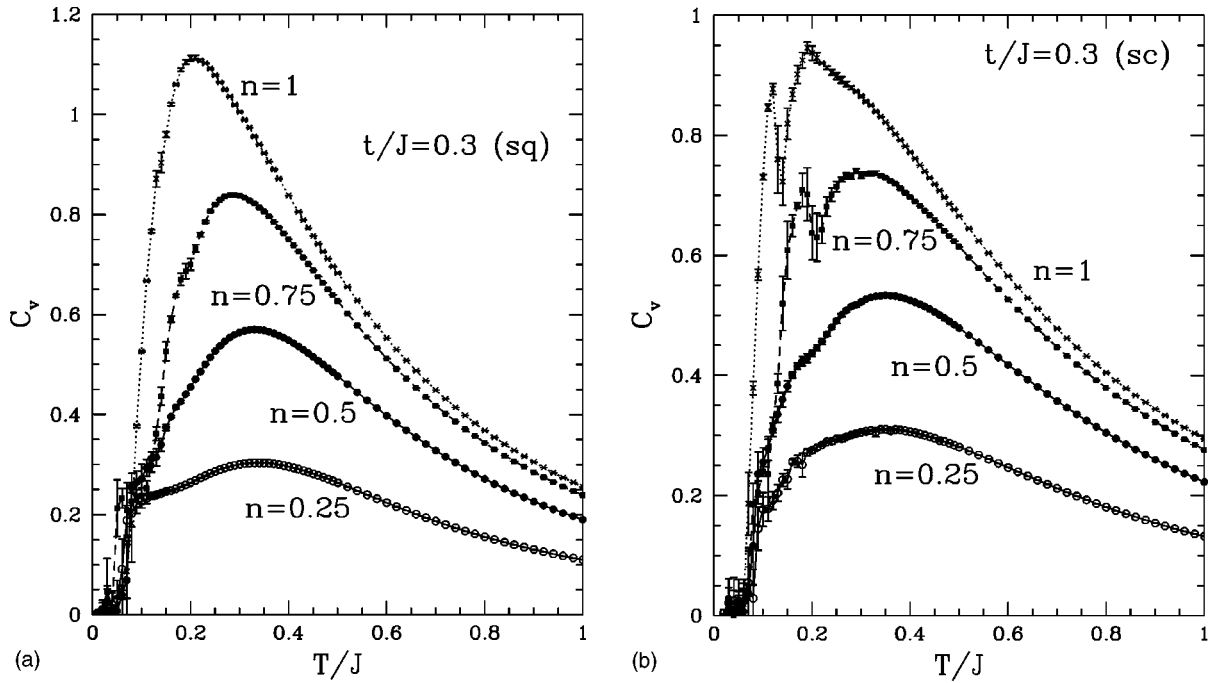
FIG. 4. The specific heat C_v vs T/J for square lattice (sq) (a) and simple cubic lattice (sc) (b) at $t/J=0.3$ for $n=1$, 0.75, 0.5, and 0.25.

tices, χ_s^{-1} appears to vanish linearly as $T \to 0$ at $n=0.5$. For the simple cubic lattice, there is some indication that the curves for χ_s^{-1} at $n=0.25$ and $n=0.1$ vanish at a small finite T, confirming a finite-temperature ferromagnetic phase. However, the analysis at low temperature is imprecise and does not allow for an accurate determination of T_c. The data for the square lattice appear to show no finite-temperature ferromagnetic transition.

Finally, in Figs. 8 and 9, we show the charge susceptibility versus temperature. The behavior is qualitatively similar to the 1D case.

V. CONCLUSIONS

We have used thermodynamic perturbation theory to investigate the antiferromagnetic Kondo lattice model at finite
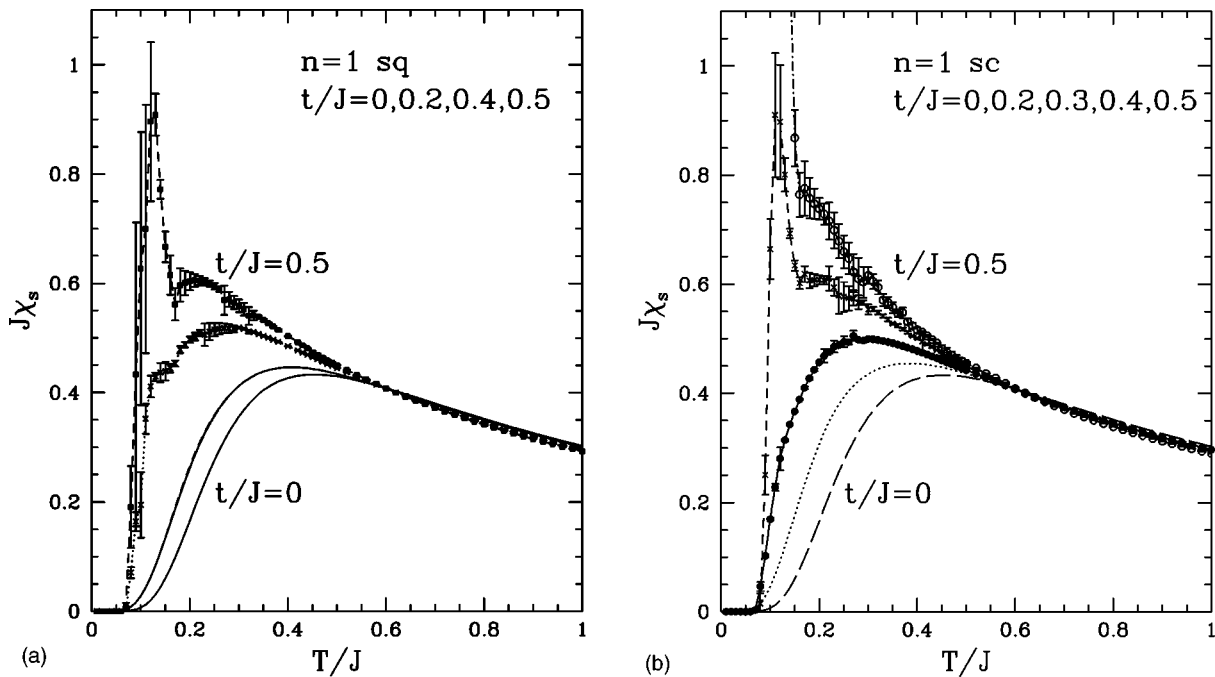
FIG. 5. The magnetic susceptibility χ_s vs T/J for square lattice (sq) (a) and simple cubic lattice (sc) (b) at $n=1$ for $t/J=0$, 0.2, 0.3, and 0.4.
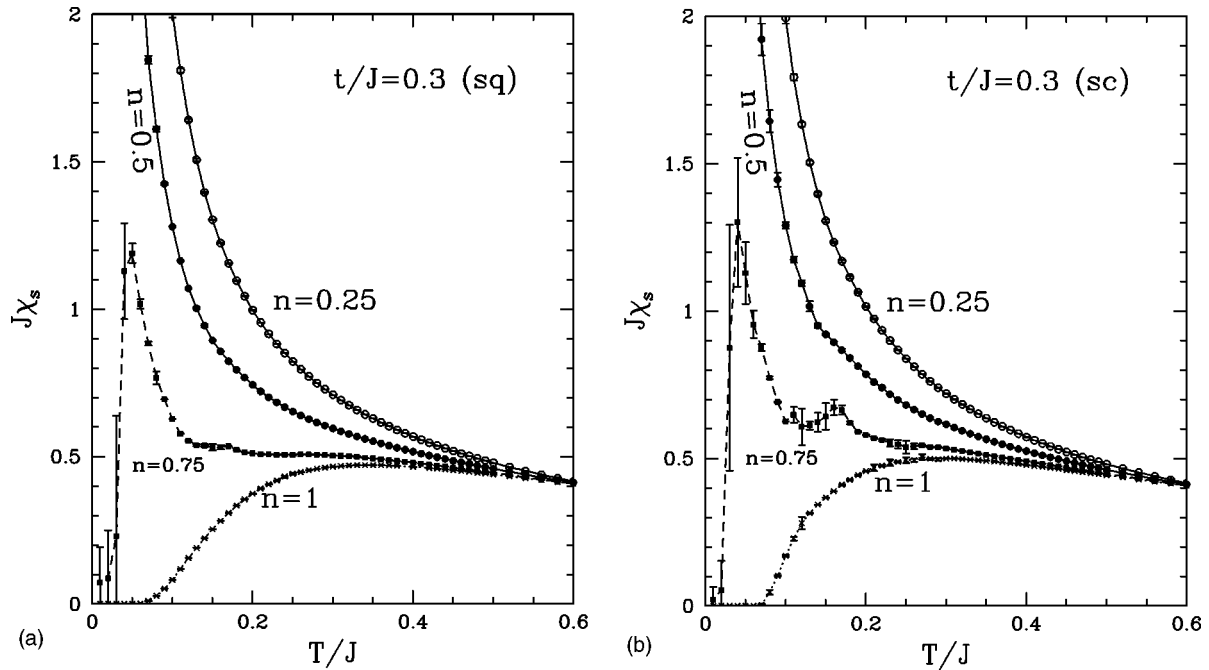
FIG. 6. The magnetic susceptibility χ_s vs T/J for square lattice (sq) (a) and simple cubic lattice (sc) (b) at $t/J=0.3$ for $n=1$, 0.75, 0.5, and 0.25.

temperatures. Our calculations focus, in particular, on the specific heat and spin and charge susceptibilities, and their variations both with the ratio t/J and with electron concentration. We have presented results for the linear chain, square lattice, and simple cubic lattice.

Overall, for the parameter region where our series can be analyzed with reasonable precision, the behavior of the three lattices is qualitatively similar. This is to be expected at mod-

erate and high temperatures. We do, however, see an indication of a finite-temperature ferromagnetic transition in three-dimensions for a small n, consistent with expectations. This is not seen in one and two dimensions.

For the linear chain, our results are in excellent agreement with the previous finite-temperature DMRG calculations[5] and serve to confirm the accuracy of both methods. There are few existing results in higher dimension and our work
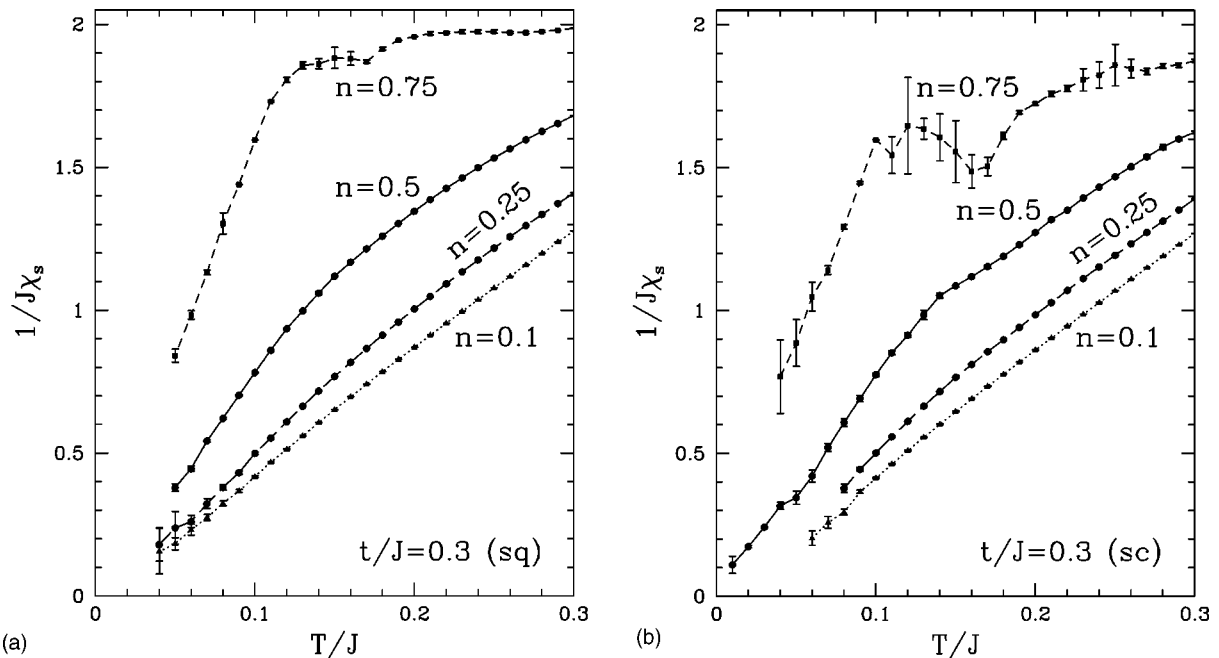
FIG. 7. The inverse of magnetic susceptibility $1/\chi_s$ vs T/J for square lattice (sq) (a) and simple cubic lattice (sc) (b) at $t/J=0.3$ for $n=0.75$, 0.5, 0.25, and 0.1.
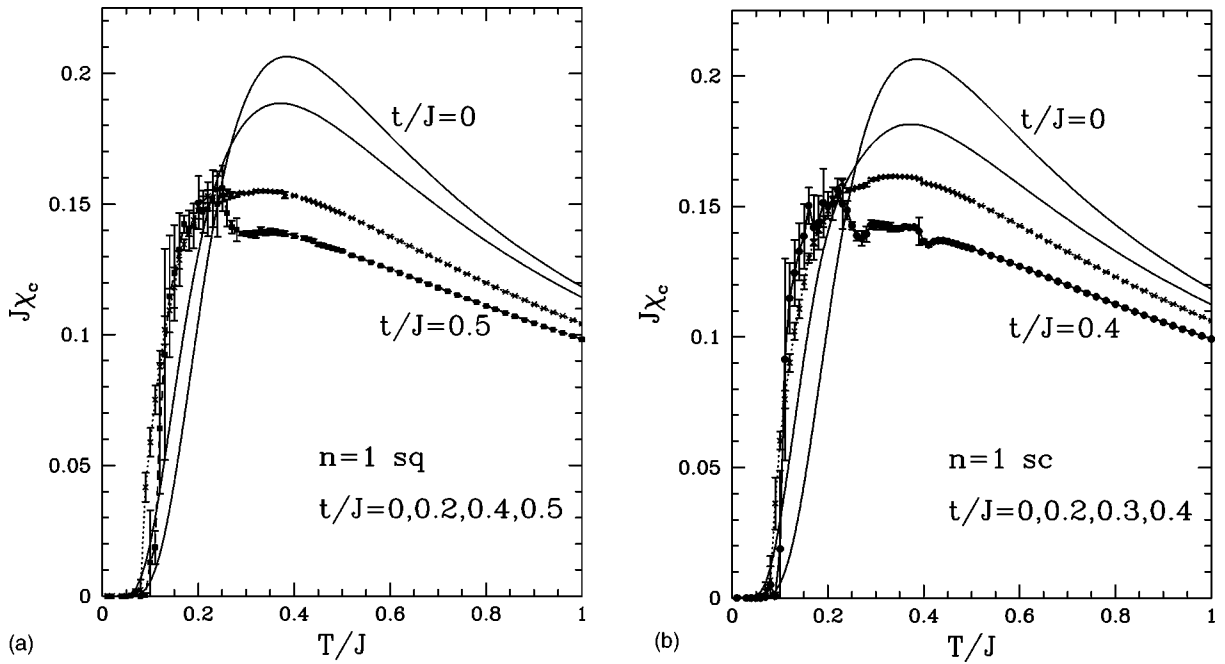
FIG. 8. The charge susceptibility χ_c vs T/J for square lattice (sq) (a) and simple cubic lattice (sc) (b) at $n=1$ for $t/J=0,0.2$, 0.3, and 0.4.

should provide a valuable benchmark for other approaches. While we have not attempted a detailed comparison on or fit to experiment, this would be possible. We plan to report results for close-packed lattices (triangular and face-centered cubic) and for the ferromagnetic Kondo lattice model elsewhere.

A calculation of the staggered spin susceptibility, along the lines above, would be possible and would be important to investigate the antiferromagnetic phase boundary. This would require substantial additional work, but we hope to do this in future work.
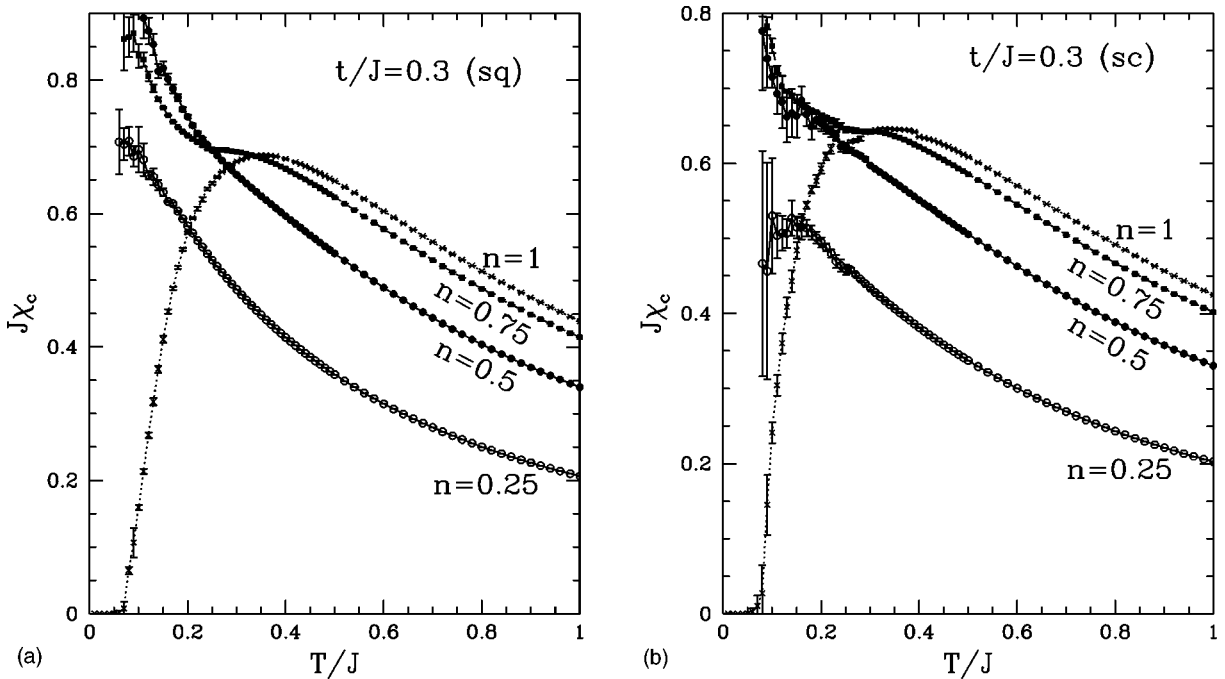
FIG. 9. The charge susceptibility χ_c vs T/J for square lattice (sq) (a) and simple cubic lattice (sc) (b) at $t/J=0.3$ for $n=1$, 0.75, 0.5, and 0.25.

tions were performed on an AlphaServer SC computer. We are grateful for the computing resources provided by the Australian Partnership for Advanced Computing (APAC) National Facility.

APPENDIX

The following high-temperature expansions up to order K^4 have been obtained from the general results. The series are expressed in terms of $K = \beta J/4$. The parameters are $\lambda = t/J$, $z =$ coordination number, p_4 is weak embedding constant of square cluster, which has value 0, 1, 3, and 12 for 1D, square lattice, simple cubic lattice, and BCC lattice, respectively, and $z_2 = 2(4 p_4 + z + z^2)/3$.

Fugacity ζ:

$$
\begin{aligned}
\zeta = \frac{n}{2-n} - \frac{n(1-n)}{2-n} &\left[\left(\frac{3}{2} + 8z\lambda^2 \right) K^2 + K^3 \right. \\
&- \frac{1}{8}(11 - 27n + 9n^2)K^4 - 4z(4-3n)\lambda^2 K^4 \\
&- 32z(1 - 6n + 3n^2)\lambda^4 K^4 \\
&\left. - 32z_2(1 + n - n^2)\lambda^4 K^4 \right] + O(K^5).
\end{aligned}
\tag{A1}
$$

Internal energy:

$$
\begin{aligned}
u/J = -\frac{1}{32}n(2-n)[&(12 + 64z\lambda^2)K \\
&+ 12K^2 - (4 - 18n + 9n^2)K^3 - 64z\lambda^2 K^3 \\
&- 256z(2 - 6n + 3n^2)\lambda^4 K^3 - 256z_2 n(2-n)\lambda^4 K^3 \\
&- 5(4 - 6n + 3n^2)K^4 - 80z\lambda^2 K^4] + O(K^5).
\end{aligned}
\tag{A2}
$$

Specific heat:

$$
\begin{aligned}
C_v/k_B = n(2-n)K^2 &\left[\left(\frac{3}{2} + 8z\lambda^2 \right) + 3K - \frac{3}{8}(4 - 18n + 9n^2) \right. \\
&\times K^2 - 24z\lambda^2 K^2 - 96z(2 - 6n + 3n^2)\lambda^4 K^2 \\
&\left. - 96z_2 n(2-n)\lambda^4 K^2 \right] + O(K^5).
\end{aligned}
\tag{A3}
$$

Magnetic susceptibility:

$$
\begin{aligned}
\beta^{-1}\chi_s = \frac{1}{4} + \frac{1}{8}n(2-n)&\left[1 - 2K - \frac{1}{4}(8 - 6n + 3n^2)K^2 \right. \\
&- 4zn(2-n)\lambda^2 K^2 + \frac{1}{3}(2 - 6n + 3n^2)K^3 \\
&+ 8zn(2-n)\lambda^2 K^3 + \frac{1}{24}(80 - 180n + 198n^2 \\
&- 108n^3 + 27n^4)K^4 + \frac{2}{3}z(12 + 10n - 41n^2 + 36n^3 \\
&- 9n^4)\lambda^2 K^4 + 16zn(2-n)(7 - 18n + 9n^2)\lambda^4 K^4 \\
&\left. - 32z_2 n(2-n)(1 - 4n + 2n^2)\lambda^4 K^4 \right] + O(K^5).
\end{aligned}
\tag{A4}
$$

Charge susceptibility:

$$
\begin{aligned}
\beta^{-1}\chi_c = \frac{1}{2}n(2-n) - n^2(2-n)^2 &\left[\left(\frac{3}{8} + 2z\lambda^2 \right)K^2 + \frac{1}{4}K^3 \right. \\
&- \frac{1}{16}(10 - 18n + 9n^2)K^4 - z(1 + 6n - 3n^2)\lambda^2 K^4 \\
&- 8z(7 - 18n + 9n^2)\lambda^4 K^4 \\
&\left. + 16z_2(1 - 4n + 2n^2)\lambda^4 K^4 \right] + O(K^5).
\end{aligned}
\tag{A5}
$$

*Electronic address: j.oitmaa@unsw.edu.au

†Electronic address: w.zheng@unsw.edu.au; URL: http://www.phys.unsw.edu.au/~zwh

[1] H. von Löhneysen, J. Phys. Condens. Matter **8**, 9689 (1996).

[2] M. Lavagna and C. Pepin, Phys. Rev. B **62**, 6450 (2000).

[3] W.H. Zheng and J. Oitmaa, preceding paper, Phys. Rev. B **67**, 214406 (2003).

[4] H. Röder, R.R.P. Singh and J. Zang, Phys. Rev. B **56**, 5084 (1997).

[5] N. Shibata, B. Ammon, M. Troyer, M. Sigrist, and K. Ueda, J. Phys. Soc. Jpn. **67**, 1086 (1998); N. Shibata and H. Tsunetsugu, ibid. **68**, 744 (1999).

[6] K. Haule, J. Bonca, and P. Prelovsek, Phys. Rev. B **61**, 2482 (2000).

[7] N. Elstner and R.R.P. Singh, Phys. Rev. B **57**, 7740 (1998).

[8] J.A. Henderson, J. Oitmaa, and M.C.B. Ashley, Phys. Rev. B **46**, 6328 (1992).

[9] Z.P. Shi, R.R.P. Singh, M.P. Gelfand, and Z. Wang, Phys. Rev. B **51**, 15630 (1995).

[10] H. Tsunetsugu, M. Sigrist, and K. Ueda, Rev. Mod. Phys. **69**, 809 (1997).

[11] A.J. Guttmann, in "*Phase Transitions and Critical Phenomena*," edited by C. Domb and J. Lebowitz (New York, Academic, 1989), Vol. 13.